Structural Characterization and Low Temperature Transport Properties of $FeSb_2$ Single Crystals Grown by Vapor Transport

R. Vasquez[1, 2, 3], A. Kiswandhi[1,4], L. Winter[1,4], J. Whalen[1], A. Ramirez[5], J. Brooks[1,4], T. Siegrist[1,2]

[1)] National High Magnetic Field Laboratory, 1800 Dirac Dr., Tallahassee, FL 32310

[2)] Department of Chemical & Biomedical Engineering, Florida State University, 2525 Dirac Dr., Tallahassee, FL 32310

[3)] International Institute for Complex Adaptive Matter, University of California, 1 Shields Avenue, Davis, CA 95616

[4)] Department of Physics, Florida State University, 77 Chieftain Way, Tallahassee, FL 32306

[5)] Baskin School of Engineering, University of California - Santa Cruz, 1156 High St., MS SOE, Santa Cruz, CA 95064

Abstract

Bulk single crystals of iron di-antimonide, $FeSb_2$, are investigated for their transport properties at low temperatures. Crystals of sizes ranging 1.5-2.5 mm are grown through chemical vapor transport (CVT) using Cl_2 as transporting agent. Cl_2 is supplied to the reaction via decomposition of $FeCl_3$ at high temperatures. ρ(T) shows semiconducting behavior with the formation of a plateau at 10K-30K, along with a hybridization gap (ε_g~6.9-7.2meV) consistent with intrinsic behavior observed in correlated materials. Resistivity increases from room temperature (RT) by 5-6 orders of magnitude, higher than previous reports. Washing crystals achieved a reduction of Cl_2 concentration and did not appear to suppress the resistivity plateau, but did result in lower overall ρ(T) increase from RT and a change in ε_g values.

Introduction

$FeSb_2$ has emerged as a potential low temperature thermoelectric material with Peltier cooling applications. It has been reported that $FeSb_2$ shows significantly enhanced thermoelectric properties at temperatures below 77K**[1]**. This underscores its potential for helium-free cooling for superconductor applications and others with cooling requirements as low as 10-15K.

$FeSb_2$ is a narrow band gap semiconductor with strong electron correlation behavior, similar to other iron-based semiconductors**[2]**. The narrow band gap in $FeSb_2$ is believed to originate from hybridization of Fe 3d orbitals with Sb 5p and 5s states, due to lattice distortions caused by edge-sharing $FeSb_6$ octahedra formed along the long axis of the unit cell**[3]**. The enhancement of thermoelectric properties has been associated to the activation of the hybridization gap (~6meV**[1]**) in the material, accompanied by large carrier mobility.

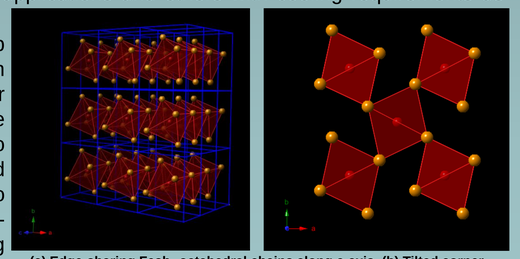

(a) Edge-sharing $Fesb_6$ octahedral chains along c-axis. (b) Tilted corner-sharing $FeSb_6$ octahedra along a-b plane

CVT Growth of $FeSb_2$ Single Crystals.

CVT Reaction Parameters	
Back-transport	24 hrs
Hot (Charge) Zone	700 ºC
Cold (Growth) Zone	650 ºC
Reaction Time	5 days
$Cl_{2(g)}$ Pressure	0.50-0.75 atm.

$FeSb_2$ growth carried out with stoichiometric amounts of elemental Sb (Sigma Aldrich, 99.9998%) and Fe (Alfa Aesar, 99.99%); mixed with anhydrous $FeCl_3$ (Sigma Aldrich, 97%). $FeCl_3$ decomposition above 315ºC provided $Cl_{2(g)}$ for Fe transport into the vapor phase**[4]**. Crystals of sizes ranging 1.5-2.5mm were synthesized.

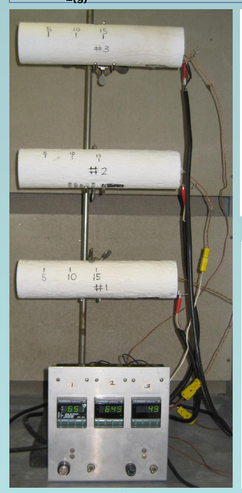

(a)

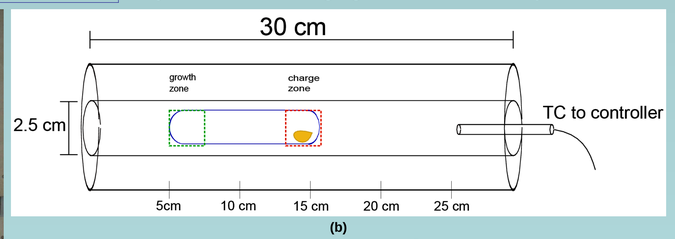

(b)

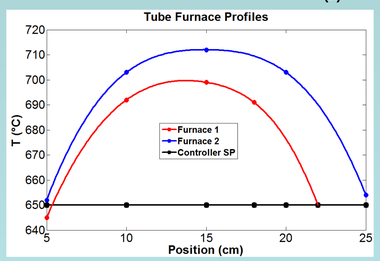

(c)

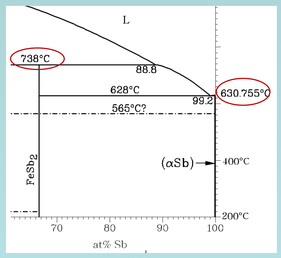

(d)

(a) Home-built synthesis setup with Watlow® tube furnaces (1 & 2). (b) Reactions vacuum-sealed in quartz ampoules to lengths corresponding to required ΔT for each furnace (c). (d) $Fesb_2$ Stability Region in Fe-Sb System [5]

Transport Properties in $FeSb_2$

ρ(T) vs. T shows semiconducting behavior in $FeSb_2$, with weak temperature dependence in the range 10K-30K, as observed previously**[1,2]**. The overall magnitude of ρ(T) increase with respect to room temperature (RT) shows sample dependence. For the first sample (batch 1) the observed increase relative to RT is nearly 2 orders of magnitude higher than previously reported**[1,2,3]**. A second measured sample (batch 2) achieves only a 3-4 order of magnitude increase.

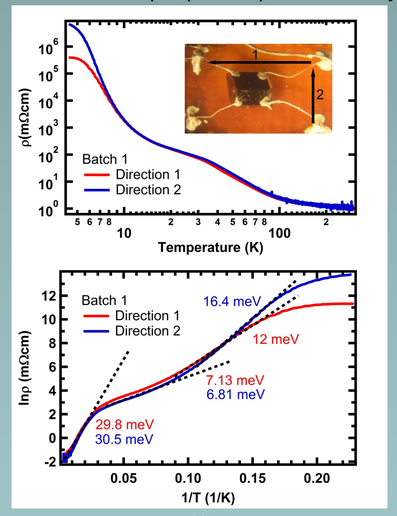

(a)

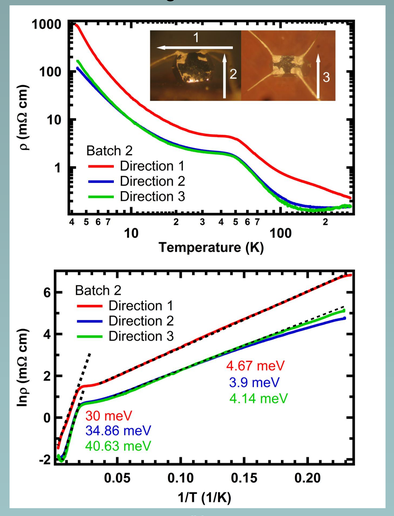

(b)

(a) Unwashed $FeSb_2$ crystal shows 5-6 order of magnitude increase in ρ(T), with ε_g consistent with previous reports[1,2]. (b) $FeSb_2$ crystal washed in water and organic solvents to remove $FeCl_3$ excess shows decrease in ρ(T) at low temperatures and a change in ε_g values.

Structural and Chemical Characterization of Crystals

Single crystal x-ray diffraction experiments conducted with an Oxford Instruments Xcalibur™2 4-Circle Kappa Single Crystal Diffractometer, Mo Kα1 (λ=0.71073 nm) source. SEM-EDS measurements conducted in a JEOL® JSM-5900 scanning electron microscope. Powder x-ray diffraction analysis confirmed phase purity of the crystals, with no secondary crystalline phases present. EDS analysis confirms $FeSb_2$ stoichiometry, with less than 0.20 at% Cl impurity.

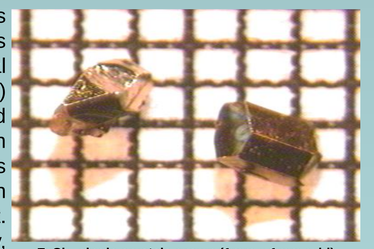

$FeSb_2$ single crystals grown (1mm x 1mm grid)

Single Crystal Diffraction Results				
Space group	Pnnm (N. 68)			
		This work	**Reference[6]**	
Lattice parameters (Å)		a = 5.8306(1) b = 6.5380(1) c = 3.1977(1)	a = 5.829(1) b = 6.535(1) c = 3.196(1)	
V (Å³)		121.90	121.74	
Z		2		
Density (g/cm³)		8.156		
μ (mm⁻¹)		27.144		
Reflections collected		7073		
R		0.0450		
Data collection range (º)		3.1095 < θ < 66.1663		
		x	**y**	**z**
Atomic Positions	**Sb**	0.1883	0.3563	0.0000
	Fe	0.0000	0.0000	0.0000

Topography in CVT-Grown $FeSb_2$ Bulk Single Crystals

Topographic studies conducted with an Asylum Research MFP-3D Atomic Force Microscope. The growth regime deviates from ideal layer-by-layer growth and instead appears to follow surface roughening behavior with multiple surface nuclei**[7]**.

$FeSb_2$ Surface Roughness		
Surface Characteristics	**Surface Area (μm²)**	**RMS (nm)**
Scattered elevations	25	17.896
Flat valley	0.09	0.442

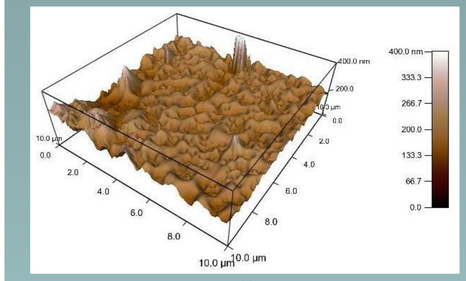

(a)

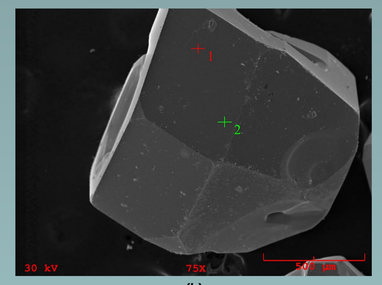

(b)

(a) $FeSb_2$ crystal surface featuring valleys and elevations. Larger peaks (~400 nm) possibly related to surface impurities or small cracks and irregularities. (b) SEM image of $FeSb_2$ single crystal showing possible irregularities on the surface.

Conclusions and Future Work

- $FeSb_2$ single crystals were successfully grown by chemical vapor transport using Cl_2 (via $FeCl_3$ decomposition above 315 ºC) as transporting agent. Structural and chemical characterization via x-ray diffraction (single crystal and powder) and SEM-EDS confirmed $FeSb_2$ stoichiometry without secondary crystalline phases present and Cl_2 impurity concentrations below 0.2 at%.
- ρ(T) measurements reveal semiconducting behavior in $FeSb_2$ with the formation of weak temperature dependent plateau in the range 10K-30K, consistent with what has been observed in previous studies. The magnitude of resistivity increase with respect to RT appears to be sensitive to post-CVT sample treatments.
- Topological studies on $FeSb_2$ single crystals show a growth environment deviating from smooth layered growth and following a surface roughening model during CVT. An RMS value of 0.44 nm was estimated for relatively flat areas on the surface.
- $FeSb_2$ samples will be further evaluated for low temperature thermoelectric performance, with Seebeck coefficient, thermal conductivity and charge carrier concentration studies currently underway. Future work also focuses on the effect of Sb-site doping on the overall improvement of key thermoelectric parameters.

References & Acknowledgements

R. V. is supported by I2CAM through NSF Grant No. DMR-0844115. A portion of this work was performed at the National High Magnetic Field Laboratory, which is supported by NSF Cooperative Agreement No. DMR-0654118, by the State of Florida, and by the DOE.

1) **A. Bentien, S. Johnsen, G. K. H. Madsen, B. B. Iversen, F. Steglich. Europhysics Letters. 2007, 80, 17008.**
2) **P. Sun, N. Oeschler, S. Johnsen, B. B. Iversen, F. Steglich. Dalton Transactions. 2009, 39(4):1012-1019.**
3) **C. Petrovic, J. W. Kim, S. L. Bud'ko, A. I. Goldman, P. C. Canfield, W. Choe, G. J. Miller. Phys Rev B. 2003, 67(15), 155205.**
4) **G. Rosenthal, R. Kershaw, A. Wold. Mat. Res. Bull. 1972, 7(5): 479-487.**
5) **T. B. Massalski, P. R. Subramanian, H. Okamoto, L. Kacprzak. Binary Alloy Phase Diagrams, 2nd ed. ASM Intl., Materials Park, OH (1990), pp. 1763-1767.**
6) **A. K. L. Fan, G. H. Rosenthal, H. L. McKinzie, A. Wold. J. Solid State Chem. 1972, 5: 136-143.**
7) **K. Nassau, J. Nassau, E. Schönherr, D. E. Ovsienko, G. A. Alfintsev, A. H. Morrish. Crystals: Growth, Properties, and Applications, Springer-Verlag, Berlin, Germany (1980), pp. 58-60.**